Chapter 11

Functionalized GaN Based Transistors For Biosensing

Stephen J. Pearton, Fan Ren and Byung Hwan Chu

Additional information is available at the end of the chapter

http://dx.doi.org/10.5772/50351

1. Introduction

The US market size of chemical sensors is projected to increase 8.6% annually to reach $6 billion in 2014. This growth will be sustained especially by high demand of biosensors for medical applications such as glucose monitoring, biomarker detection for infectious disease and cancer diagnosis. In addition, there will be strong demand in biodefense, environmental monitoring, food, and pharmaceutical industries. The biosensor market is forecast to reach $4.4 billion in 2014 in the US [1].

There is interest in developing sensors that could be used in point-of-care applications or on-field measurements. These sensors need to have high precision, compact size, fast response time and be sensitive to small amount of biological material. Field effect transistor structures (FETs) are promising for these applications. In a standard FET, the size and shape of the conductive channel between the source and drain terminals is controlled by an electrode that applies gate voltage. In place of the electrode, chemical characteristics of the active area could also play a crucial role in controlling the performance behaviors of the device. This property makes semiconductors ideal materials for sensors in many chemical and biochemical systems. Compared to methods such as protein assays [2], there is no need for optical components to translate the surface binding phenomena into a readable signal. Semiconductor properties including, surface current, potential, and impedance characteristics can be used to directly measure chemical or physical stimuli on the semiconductor surface [3-10]. Handheld, wireless-capable medical sensors are attractive for reducing financial and emotional cost of false-positive tests. The ability to make robust, inexpensive sensor arrays using semiconductor technology is one of the main driving forces behind this work. A typical semiconductor-based bio-sensor consists of a bio-receptor and transducer, which is generally a gateless field effect transistor structure. The bio-receptor is typically an enzyme or antibody layer attached to the gate of the FET.

To date, silicon-based sensors have been the main platform due to their low cost and maturity as well as the extensive experience base for chemical treatments on silicon oxide or glass. A drawback with Si sensors is that they generally cannot operate under harsh conditions of elevated temperature and /or pressure, and they are susceptible to degradation in chemically corrosive environments. This has led to interest in the use of GaN-based semiconductors as alternatives to silicon because of their greater chemical inertness in acidic and basic solutions, higher temperature of operation and ability to also emit and blue and ultraviolet light that can be used for fluorescence detection of particular bio-species. Other GaN applications already commercialized include blue/violet/white/UV Light Emitting Diodes (LEDs) used in traffic stoplights and full color displays, blue light lasers, which are employed in high density CD-ROM storage, and high resolution printers, high power microwave transistors with applications in new generations of radar and cell phone systems and low noise, radiation hard transistors for use in high temperature sensors and space-flight instrumentation.

In the area of detection of medical biomarkers, many different methods, including enzyme-linked immunsorbent assay (ELISA), particle-based flow cytometric assays, electrochemical measurements based on impedance and capacitance, electrical measurement of microcantilever resonant frequency change, and conductance measurement of semiconductor nanostructures. gas chromatography (GC), ion chromatography, high density peptide arrays, laser scanning quantitiative analysis, chemiluminescence, selected ion flow tube (SIFT), nanomechanical cantilevers, bead-based suspension microarrays, magnetic biosensors and mass spectrometry (MS) have been employed [1,2]. Depending on the sample condition, these methods may show variable results in terms of sensitivity for some applications and may not meet the requirements for a handheld biosensor. Most of the techniques mentioned earlier such as ELISA possesses a major limitation in that only one analyte is measured at a time. Particle-based assays allow for multiple detection by using multiple beads but the whole detection process is generally longer than 2 hours, which is not practical for in-office or bedside detection. Electrochemical devices have attracted attention due to their low cost and simplicity, but significant improvements in their sensitivities are still needed for use with clinical samples. Microcantilevers are capable of detecting concentrations of 10 pg/ml, but suffer from an undesirable resonant frequency change due to the viscosity of the medium and cantilever damping in the solution environment. In clinical settings, biomarkers for a particular disease state can be used to determine the presence of disease as well as its progress.

A promising FET sensing technology utilizes AlGaN/GaN high electron mobility transistors (HEMTs). HEMT structures have been developed for use in microwave power amplifiers due to their high two dimensional electron gas (2DEG) mobility and saturation velocity. The conducting 2DEG channel of AlGaN/GaN HEMTs is very close to the surface and extremely sensitive to adsorption of analytes. HEMT sensors can be used for detecting pH values, proteins, and DNA.The GaN materials system is attracting much interest for commercial applications of green, blue, and UV light emitting diodes (LEDs), laser diodes as well as high speed and high frequency power devices. Due to the wide-bandgap nature of the material, it is very thermally stable, and electronic devices can be operated at temperatures up to 500 ºC. The GaN based materials are also chemically stable, and no known wet chemical etchant can etch

http://dx.doi.org/10.5772/50351

these materials; this makes them very suitable for operation in chemically harsh environments. Due to the high electron mobility, GaN material based high electron mobility transistors (HEMTs) can operate at very high frequency with higher breakdown voltage, better thermal conductivity, and wider transmission bandwidths than Si or GaAs devices [3-10].

The high electron sheet carrier concentration of nitride HEMTs is induced by piezoelectric polarization of the strained AlGaN layer in the hetero-junction structure of the AlGaN/GaN HEMT and the spontaneous polarization is very large in wurtzite III-nitrides. This provides an increased sensitivity relative to simple Schottky diodes fabricated on GaN layers or FETs fabricated on the AlGaN/GaN HEMT structure. The gate region of the HEMT can be used to modulate the drain current in the FET mode or use as the electrode for the Schottky diode. A variety of gas, chemical and health-related sensors based on HEMT technology have been demonstrated with proper surface functionalization on the gate area of the HEMTs, including the detection of hydrogen, mercury ions, prostate specific antigen (PSA), DNA, and glucose.

In this chapter, we discuss progress in functionalization of these sensors for applications in detection of gases, pH measurement, biotoxins and other biologically important chemicals and the integration of these sensors into wireless packages for remote sensing capability.

2. Sensor Functionalization

One drawback of HEMT sensors is a lack of selectivity to different analytes due to the chemical inertness of the HEMT surface. This can be solved by surface modification with detecting receptors. Sensor devices should be usable with a variety of fluids having environmental and bodily origins, including saliva, urine, blood, and breath. For use with exhaled breath, the device may include a HEMT bonded on a thermo-electric cooling device, which assists in condensing exhaled breath samples. One of the key technical challenges in fabricating hybrid biosensors is the junction between biological macromolecules and the inorganic scaffolding material (metals and semiconductors) of the chip. For actual device applications, it is often necessary to selectively modify a surface at micro- and even nano-scale, sometimes with different surface chemistry at different locations. In order to enhance detection speed, especially at very low analyte concentration, the analyte should be delivered directly to the active sensing areas of the sensors. A common theme for bio/chem sensors is that their operation often incorporates moving fluids. For example, sensors must sample a stream of air or water to interact with the specific molecules they are designed to detect.

The general approach to detecting biological species using a semiconductor sensor involves functionalizing the surface (eg. the gate region of an ungated field effect transistor structure) with a layer or substance which will selectively bind the molecules of interest. In applications requiring less specific detection, the adsorption of reactive molecules will directly affect the surface charge and affect the near-surface conductivity. In their simplest form, the sensor consists of a semiconductor film patterned with surface electrodes and often heated to temperatures of a few hundred degrees Celsius to enhance dissociation of molecules on the exposed surface. Changes in resistance between the electrodes signal the adsorption of reactive molecules. It is desirable to be able to use the lowest operating temperature to maximize battery life in hand-held detection instruments.

Since GaN-based material systems are chemically stable, this should minimize degradation of adsorbed cells. The bond between Ga and N is ionic and proteins can easily attach to the GaN surface. This is one of the key factors for making a sensitive biosensor with a useful lifetime. HEMT sensors have been used for detecting gases, ions, pH values, proteins, and DNA temperature with good selectivity by the modification of the surface in the gate region of the HEMT. The 2DEG channel is connected to an Ohmic-type source and drain contacts. The source-drain current is modulated by a third contact, a Schottky-type gate, on the top of the 2DEG channel. For sensing applications, the third contact is affected by the sensing environment, i.e. the sensing targets changes the charges on the gate region and behave as a gate. When charged analytes accumulate on the gate area, these charges form a bias and alter the 2DEG resistance. This electrical detection technique is simple, fast, and convenient. The detecting signal from the gate is amplified through the drain-source current and makes this sensor very sensitive for sensor applications. The electric signal also can be easily quantified, recorded and transmitted, unlike fluorescence detection methods which need human inspection and are difficult to precisely quantify and transmit the data. Table 1 shows a summary of surface functional layers used with HEMT sensors for selective detection of various gases, toxins, cancers and biomarkers, heavy metals, pressure changes and marine pathogens.

3. pH Sensors

An important aspect of biosensing, particularly for health monitoring, is the need to monitor the concentration of several different species for calibration purposes or conditions such as pH. which can also be used to calibrate samples of breath condensate. The glucose oxidase enzyme (GOx) is commonly used in biosensors to detect levels of glucose for diabetics. However, the activity of GOx is highly dependent on the pH value of the solution. The pH value of a typical healthy person is between 7 and 8. This can vary significantly depending on the health condition of each individual, e.g. the pH value for patients with acute asthma was reported as low as 5.23 + 0.21 (n=22) as compared to 7.65 + 0.20 (n=19) for the control subjects. To achieve accurate glucose concentration measurement with immobilized GO_x, it is necessary to determine the pH value and glucose concentration with an integrated pH and glucose sensor.

The measurement of pH is needed in many applications, including medicine, biology, food and environmental science and oceanography. Solutions with a pH less than 7 are acidic and solutions with a pH greater than 7 are basic or alkaline. Ungated AlGaN/ GaN HEMTs exhibit large changes in current upon exposing the gate region to polar liquids [6]. The polar nature of electrolyte introduced to the surface produces a change of surface charge and hence surface potential at the semiconductor /liquid interface. The use of Sc_2O_3 gate dielectric in the gate region produces superior results to either a native oxide or UV ozone-induced oxide. The ungated HEMTs with Sc_2O_3 in the gate region exhibited a linear change in current between pH 3-10 of 37μA/pH. Figure 1 shows a scanning electron microscopy (SEM) image (top) and a cross-sectional schematic (bottom) of the completed device. The gate dimension of the device is 2 × 50 μm^2. The pH solution was applied using a syringe autopipette (2-20ul).

http://dx.doi.org/10.5772/50351

Detection	Mechanism	Surface Functionalization	Detection Limit
1. Gases			
H_2	Catalytic dissociation	Pd,Pt	10 ppm
CO_2	Absorption of water/ charge	Polyethylenimine/starch	1%
CO	Charge transfer	ZnO nanowires	50 ppm
O_2	Oxidation	InZnO	5%
2.Toxins			
Botulinum	Antibody	Thioglycolic acid/antibody	1 ng/ml
Anthrax Protective Antigen	Antibody	Thioglycolic acid/antibody	2µg/ml
3. Cancers			
Breast cancer	Antibody	Thioglycolic acid/c-erbB antibody	
Prostate Specific Antigen	Antibody	Carboxylate succimdyl ester/PSA antibody	10 pg/ml
4. Biomarkers			
DNA	Hybridization	3′-thiol-modified oligonuceotides	
Chloride ions	Anodization	Ag/AgCl electrodes, InN	10^{-8} M
Lactic acid	LOX immobilization	ZnO nanorods	167 nM
Glucose	GOX immobilization	ZnO nanorods	0.5 nM
Proteins	Conjugation/hybridization	Aminoprpoylsilane/biotin	
pH	Absorption of polar molecules	Sc_2O_3 , ZnO	±0.01
KIM-1	Antibody	KIM-1 Antibody	1 ng/ml
Traumatic Brain Injury	Antibody	TBI Antibody	1 µg/ml
5. Heavy Metals			
Hg+ with Na, Pb, Mg ions	Chelation	Thioglycolic acid/Au	1 nM
6. Marine pathogens/diseases			
Perkinsus marinus	Antibody	Thioglycolic acid/anti-P marinus antibody	
Vitellogenin	Antibody	Thioglycolic acid/anti-vitellogenin antibodies	1% serum of 4 µg/ml

Table 1. Summary of surface functional layers used with HEMT sensors.

The pH solution made by the titration method using HCl, NaOH and distilled water. The electrode was a conventional Acumet standard Ag/AgCl electrode. Figure 2 shows the current at a bias of 0.25V as a function of time from HEMTs with Sc_2O_3 in the gate region exposed for 150s to a series of solutions whose pH was varied from 3-10. The current is increased upon exposure to these polar liquids as the pH is decreased. The change in current was 37 μA/pH. The HEMTs show stable operation with a resolution of ~0.1 pH over the entire pH range.

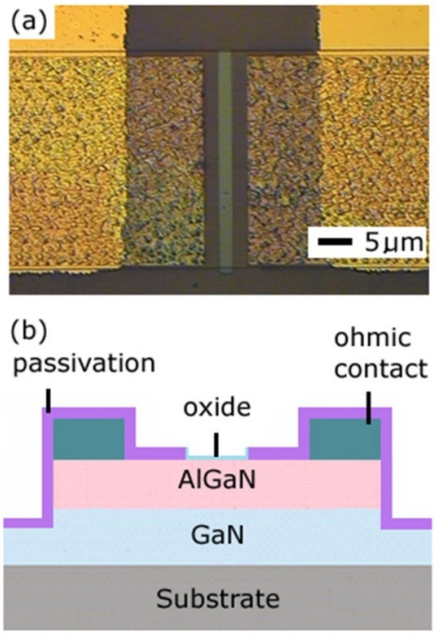

Figure 1. SEM and schematic of gateless HEMT.

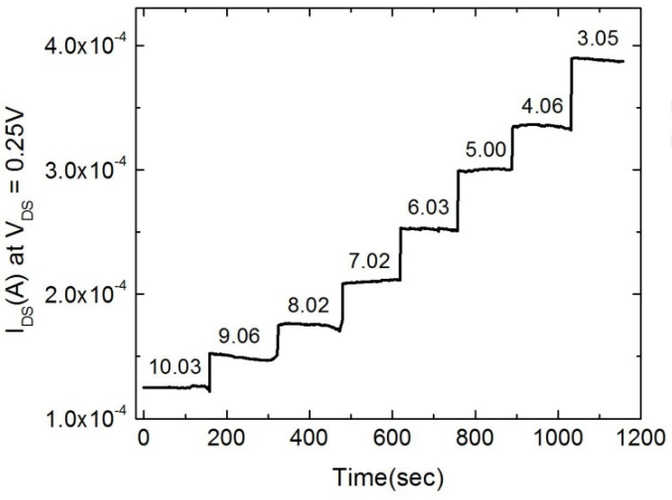

Figure 2. Change in current of HEMT with pH from 3-10.

http://dx.doi.org/10.5772/50351

4. Clinically Relevant Gas Detection

(i) O_2 Sensing

The current technology for O_2 measurement, referred to as oximetry, is small and convenient to use [11,12]. However, the O_2 measurement technology does not provide a complete measure of respiratory sufficiency. A patient suffering from hypoventilation (poor gas exchange in the lungs) given 100% oxygen can have excellent blood oxygen levels while still suffering from respiratory acidosis due to excessive CO_2. The O_2 measurement is also not a complete measure of circulatory sufficiency. If there is insufficient blood flow or insufficient hemoglobin in the blood (anemia), tissues can suffer hypoxia despite high oxygen saturation in the blood that does arrive. The current oxide-based O_2 sensors can operate at very high temperatures, such as the commercialized solid electrolyte ZrO_2 (700ºC) or the semiconductor metal oxides such as TiO_2, Nb_2O_5, $SrTiO_3$, and CeO_2 (>400ºC). However, it remains important to develop a low operation temperature and high sensitivity O_2 sensor to build a small, portable and low cost O_2 sensor system for biomedical applications.

Oxide-based materials are widely used and studied for oxygen sensing because of their low cost and good reliability. The commercialized solid electrolyte ZrO_2 has been widely used in automobiles for oxygen sensing in combustion processes. The electrolyte metal oxide oxygen sensor usually uses a reference gas and operates at high temperature (700˚C) [12]. The semiconductor metal oxides mentioned above do not need the reference gas, but they still need to be operated at a considerably high temperature (>400˚C) in order to reach high sensitivity, which means a high power consumption for heating up the sensors [13-15]. For biomedical applications, such as monitoring oxygen in the breath for a lung transplant patient, a portable and low power consumption O_2 sensor system is needed. Therefore, it is crucial to develop a low operating temperature and high sensitivity O_2 sensor for those applications.

The conductivity mechanism of most metal oxides based semiconductors results from electron hopping from intrinsic defects in the oxide film and these defects are related to the oxygen vacancies generated during oxide growth [13-15]. Typically, the higher the concentration of oxygen vacancies in the oxide film, the more conductive is the film. InZnO (IZO) films have been used in fabricating thin film transistors and the conductivity of the IZO is also found to depend on the oxygen partial pressure during the oxide growth. The IZO is a good candidate for O_2 sensing applications.

The schematic of the oxygen sensor based on oxide-functionalized HEMTs is shown at the top of Figure 3. The bottom part of the figure shows the device had a strong response when it was tested at 120˚C in pure nitrogen and pure oxygen alternately at a bias voltage of 3V. When the device was exposed to oxygen, the drain-source current decreased, whereas when the device was exposed to nitrogen, the current increased. The IZO film provides a high oxygen vacancy concentration, which makes the film readily sense oxygen and create a potential on the gate area of the AlGaN/GaN HEMT. A sharp drain-source current change demonstrates the combination of the advantage of the high electron mobility of the HEMT and the high oxygen vacancy concentration of the IZO film. Because of these advantages, this oxygen sensor can operate with a high sensitivity at a relatively low temperature compared to many oxide-based oxygen sensors which operate from 400˚C to 700˚C. The combination of IZO films and the AlGaN / GaN HEMT allows realization of low operation temperature and low power consumption oxygen sensor.

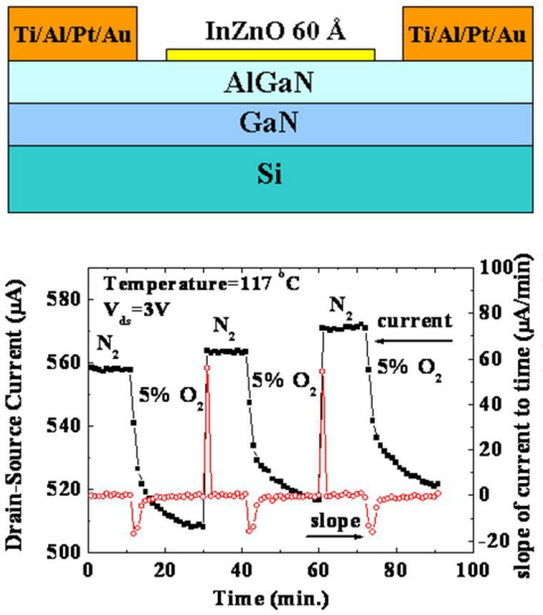

Figure 3. Schematic of AlGaN/GaN HEMT based O2 sensor (top) and drain current of IZO functionalized HEMT sensor measured at fixed source-drain during the exposure to different O2 concentration ambients. The drain bias voltage was 0.5 V and measurements were conducted at 117 oC.

(ii) CO_2Sensing

The detection of carbon dioxide (CO_2) gas is important for global warming, biological and health-related applications such as indoor air quality control, process control in fermentation, and in the measurement of CO_2 concentrations in patients' exhaled breath with lung and stomach diseases. In medical applications, it can be critical to monitor the CO_2 and O_2 concentrations in the circulatory systems for patients with lung diseases in the hospital. The current technology for CO_2 measurement typically uses IR instruments, which can be very expensive and bulky [16-22].

The most common approach for CO_2 detection is based on non-dispersive infrared (NDIR) sensors, which are the simplest of the spectroscopic sensors. The best detection limits for the NDIR sensors are currently in the range of 20-10,000 ppm. The key components of the NDIR approach are an infrared (IR) source, a light tube, an interference filter, and an infrared (IR) detector. In operation, gas enters the light tube. Radiation from the IR light source passes through the gas in the light tube to impinge on the IR detector. The interference filter is positioned in the optical path in front of the IR detector such that the IR detector receives the radiation wavelength that is strongly absorbed by the gas whose concentration is determined while filtering out the unwanted wavelengths. The IR detector produces an electrical signal that represents the intensity of the radiation impinging upon it. It is generally considered that the NDIR technology is limited by power consumption and size.

In recent years, monomers or polymers containing amino-groups, such as tetrakis (hydroxyethyl)ethylenediamine, tetraethylene-pentamine and polyethyleneimine (PEI) have been used for CO_2 sensors to overcome the power consumption and size issues found in the NDIR approach [21-24]. Most of the monomers or polymers are utilized as coatings of surface acous-

http://dx.doi.org/10.5772/50351

tic wave transducers. The polymers are capable of adsorbing CO_2 and facilitating a carbamate reaction. PEI has also been used as a coating on carbon nanotubes for CO_2 sensing by measuring the conductivity of nanotubes upon exposing to the CO_2 gas. For example, CO_2 adsorbed by a PEI coated nanotube portion of a NTFET (nanotube field effect transistor) sensor lowers the total pH of the polymer layer and alters the charge transfer to the semiconducting nanotube channel, resulting in the change of NTFET electronic characteristics [25-28].

The HEMT-based device relies on the interaction between CO_2 and amino group-containing compounds. Addition of starch into the PEI enhances the absorption of the water molecules into the PEI/starch thin film. The reaction mechanism is expected to be that primary amine groups, $-NH_2$, on the PEI main chain react with CO_2 and water forming $–NH_3^+$ ions and the CO_2 molecule became OCOOH- ions. Thus, the charges, or the polarity, on the PEI main chain were changed. The electrons in the two-dimensional electron gas (2DEG) channel of the AlGaN/GaN HEMT are induced by piezoelectric and spontaneous polarization effects. The PEI/starch was coated on the gate region of the HEMT. The charges of the PEI changed through the reactions between $-NH_2$ and CO_2 as well as water molecules are then transduced into a change in the concentration of the 2DEG in the AlGaN/GaN HEMTs.

PEI/starch functionalized HEMT sensors were found to be capable of measuring different CO_2 concentration at temperatures as low as 108 C and a fixed source-drain bias voltage of 0.5 V. The current increased with the introduction of CO_2 gas. This was due to the net positive charges increased on the gate area, thus inducing electrons in the 2DEG channel. The response to CO_2 gas had a wide dynamic range from 0.9% to 50%. Higher CO_2 concentrations were not tested because there is little interest in these for medical related applications. The response times were on the order of 100 seconds. The drain current changes were linearly proportional to the CO_2 concentration for all the tested temperatures and higher sensitivity for the higher testing temperatures. There was a noticeable change of the sensitivity from the sensors tested at 61 C to those tested at 108 C. The sensors exhibited reversible and reproducible characteristics [29].

5. Biotoxin Sensors

Reliable detection of biological agents in the field and in real time is challenging. The objective of this application is to develop and test a wireless sensing technology for detecting logicalb toxins. A significant issue is the absence of a definite diagnostic method and the difficulty in differential diagnosis from other pathogens that would slow the response in case of a terror attack. Our aim is to develop reliable, inexpensive, highly sensitive, handheld sensors with response times on the order of a few seconds, which can be used in the field for detecting biological toxins.

The current methods for toxin sensing in the field are generally not suited for field deployment and there is a need for new technologies. The current methods are impractical because such tests can only be carried out at centralized locations, and are too slow to be of practical value in the field. These still tend to be the methods of choice in current detection of toxins, eg. the standard test for botulinum toxin detection is the ‘mouse assay’, which relies on the death of mice as an indicator of toxin presence [30].

(i) Botulinum

Antibody-functionalized Au-gated AlGaN/GaN HEMTs show great sensitivity for detecting botulinum toxin. The botulinum toxin was specifically recognized through botulinum antibody, anchored to the gate area, as shown in Figure 4. We investigated a range of concentrations from 0.1 ng/ml to 100 ng/ml. The source and drain current from the HEMT were measured before and after the sensor was exposed to 100 ng/ml of botulinum toxin at a constant drain bias voltage of 500 mV. Figure 5 (top) shows a real time botulinum toxin detection in PBS buffer solution using the source and drain current change with constant bias of 500 mV. No current change can be seen with the addition of buffer solution around 100 seconds, showing the specificity and stability of the device. In clear contrast, the current change showed a rapid response in less than 5 seconds when target 1 ng/ml botulinum toxin was added to the surface. The abrupt current change due to the exposure of botulinum toxin in a buffer solution was stabilized after the botulinum toxin thoroughly diffused into the buffer solution. Different concentrations (from 0.1 ng/ml to 100 ng/ml) of the exposed target botulinum toxin in a buffer solution were detected. The sensor saturates above 10ng/ml of the toxin. The limit of detection of this device was below 1 ng/ml of botulinum toxin in PBS buffer solution. The source-drain current change was nonlinearly proportional to botulinum toxin concentration, as shown in Figure 5 (bottom). Figure 6 shows a real time test of botulinum toxin at different toxin concentrations. This result demonstrates the real-time capabilities of the chip [31]. These tests are typical for our sensors, to demonstrate their quick response to different concentrations.

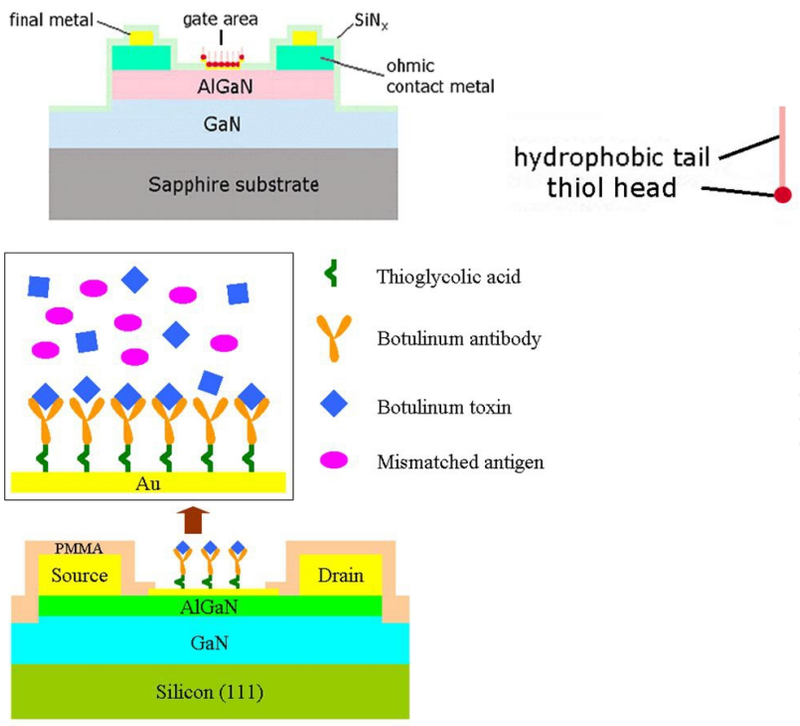

Figure 4. Schematic of AlGaN/GaN HEMT. The Au-coated gate area was functionalized with thioglycolic acid for botulinum detection.

http://dx.doi.org/10.5772/50351

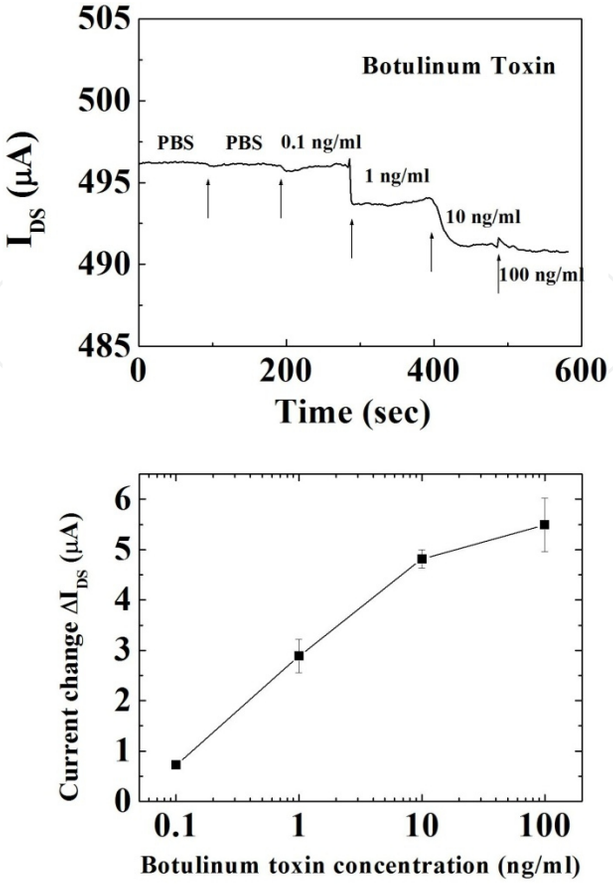

Figure 5. Drain current of an AlGaN/GaN HEMT versus time for botulinum toxin from 0.1 ng/ml to 100 ng/ml (top) and change of drain current versus different concentrations from 0.1 ng/ml to 100 ng/ml of botulinum toxin (bottom).

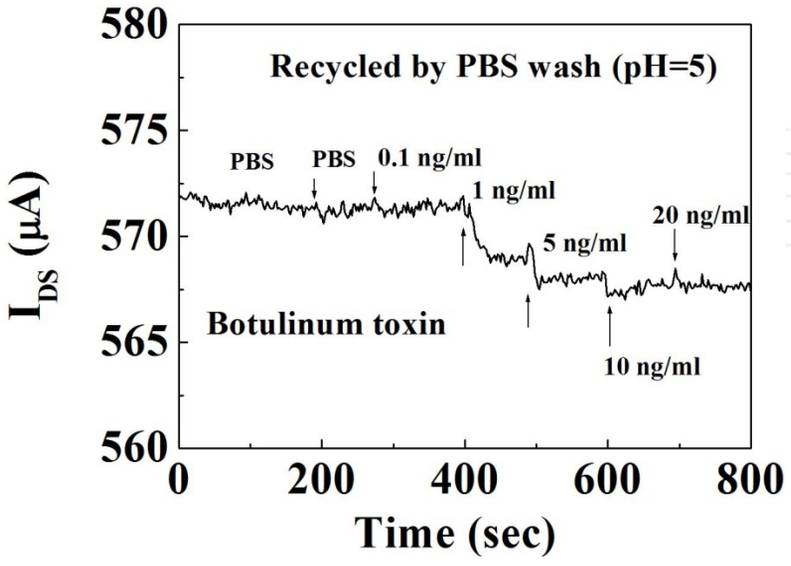

Figure 6. Real-time test from a used botulinum sensor washed with PBS in pH 5 to refresh the sensor.

6. Biomedical Applications

(i) Glucose

AlGaN/GaN HEMTs can be used for measurements of pH in exhaled breath condensate (EBC) and glucose, through integration of the pH and glucose sensor onto a single chip and with additional integration of the sensors into a portable, wireless package for remote monitoring applications [9,32]. The glucose was sensed by ZnO nanorod functionalized HEMTs with glucose oxidase enzyme localized on the nanorods. Figure 7 shows an optical microscope image of an integrated pH and glucose sensor chip and cross-sectional schematics of the completed pH and glucose device. The gate dimension of the pH sensor device and glucose sensors was 20 × 50 μm^2.

For the glucose detection, an array of 20-30 nm diameter and 2 μm tall ZnO nanorods were grown on the 20 × 50 μm^2 gate area. The lower right inset in Figure 7 shows closer view of the ZnO nanorod arrays grown on the gate area. The ZnO nanorod matrix provides a microenvironment for immobilizing negatively charged glucose oxidase (GO_x) while retaining its bioactivity, and passes charges produced during the GO_x and glucose interaction to the AlGaN/GaN HEMT. The GOx solution was prepared with concentration of 10 mg/mL in 10 mM phosphate buffer saline. After fabricating the device, 5 μl GO_x solution was precisely introduced to the surface of the HEMT using a pico-liter plotter. The sensor chip was kept at 4 °C in the solution for 48 hours for GO_x immobilization on the ZnO nanorod arrays followed by an extensively washing to remove the un-immobilized GO_x.

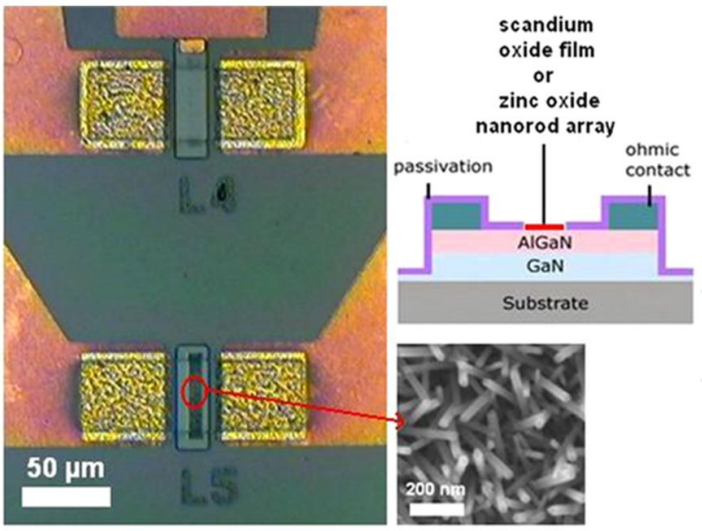

Figure 7. SEM image of an integrated pH and glucose sensor. The insets show a schematic cross-section of the pH sensor and also an SEM of the ZnO nanorods grown in the gate region of the glucose sensor.

To take the advantage of quick response (less than 1 sec) of the HEMT sensor, a real-time EBC collector is needed. The amount of the EBC required to cover the HEMT sensing area is very small. To condense 3 μl of water vapor, only ~ 7 J of energy need to be removed for

http://dx.doi.org/10.5772/50351

each tidal breath, which can be easily achieved with a thermal electric module, a Peltier device. The AlGaN/GaN HEMT sensor is directly mounted on the top of the Peltier unit, which can be cooled to precise temperatures by applying known voltages and currents to the unit. During our measurements, the hotter plate of the Peltier unit was kept at 21°C, and the colder plate was kept at 7 °C by applying bias of 0.7 V at 0.2 A. The sensor takes less than 2 sec to reach thermal equilibrium with the Peltier unit. This allows the exhaled breath to immediately condense on the gate region of the HEMT sensor.

The HEMT sensors were not sensitive to switching of N_2 gas, but responded to applications of exhaled breath pulse inputs from a human test subject, The principal component of the EBC is water vapor, which represents nearly all of the volume (>99%) of the fluid collected in the EBC. The measured current change of the exhale breath condensate shows that the pH values are within the range between pH 7 and 8. This range is the typical pH range of human blood. The sensors do not respond to glucose unless the enzyme is present, as shown in Figure 8. Although measuring the glucose in the EBC is a noninvasive and convenient method for the diabetic application, the activity of the immobilized GO_x is highly dependent on the pH value of the solution. The GOx activity can be reduced to 80% for pH = 5 to 6. If the pH value of the glucose solution is larger than 8, the activity drops off very quickly [15]. When the glucose sensor was used in a pH controlled environment, the drain current stayed fairly constant. The human pH value can vary significantly depending on the health condition. Since we cannot control the pH value of the EBC samples, we needed to measure the pH value while determining the glucose concentration in the EBC. With the fast response time and low volume of the EBC required for HEMT based sensor, a handheld and real-time glucose sensing technology can be realized.

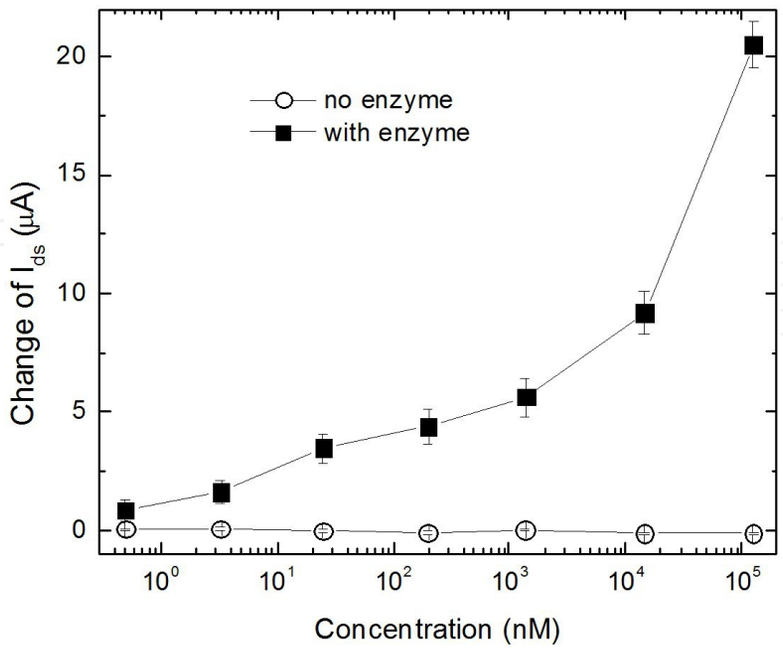

Figure 8. Change in drain-source current in HEMT glucose sensors with and without localized enzyme.

(ii) Prostate Cancer Detection

Prostate cancer is the second most common cause of cancer death among men in the United States and 1 in 6 men will be diagnosed with prostate cancer during his lifetime [3,33,34]. The most commonly used serum marker for diagnosis of prostate cancer is prostate specific antigen (PSA). Prostate cancer can often be found early by testing the amount of (PSA in the patient's blood. It can also be detected on a digital rectal exam (DRE). Most men have PSA levels under 4 nanograms per milliliter of blood. When prostate cancer develops, the PSA level usually goes up above 4 nanograms per milliliter; however, about 15% of men with a PSA below 4 will have prostate cancer on biopsy. Generally PSA testing approaches are costly, time-consuming and need sample transportation.

Antibody functionalized Au-gated AlGaN/GaN HEMTs shown schematically in Figure 9 were found to be effective for detecting PSA at low concentration levels. The PSA antibody was anchored to the gate area through the formation of carboxylate succinimdyl ester bonds with immobilized thioglycolic acid. The HEMT drain-source current showed a response time of less than 5 seconds when target PSA in a buffer at clinical concentrations was added to the antibody-immobilized surface. The devices could detect a range of concentrations from 1 μg/ml to 10 pg/ml. The lowest detectable concentration was two orders of magnitude lower than the cut-off value of PSA measurements for clinical detection of prostate cancer. Figure 10 shows the real time PSA detection in PBS buffer solution using the source and drain current change with constant bias of 0.5V[42]. No current change can be seen with the addition of buffer solution or nonspecific bovine serum albumin (BSA), but there was a rapid change when10 ng/ml PSA was added to the surface. The abrupt current change due to the exposure of PSA in a buffer solution could be stabilized after the PSA diffused into the buffer solution. The ultimate detection limit appears to be a few pg/ml [3].

(iii) Breast Cancer

The most effective and widely used diagnostic exam for breast cancer, the mammogram, is potentially harmful due to radiation exposure. Currently, the overwhelming majority of patients are screened for breast cancer by mammography [35-40]. This procedure involves a high cost to the patient and is invasive (radiation) which limits the frequency of screening. Breast cancer is currently the most common female malignancy in the world, representing 7% of the more than 7.6 million cancer-related deaths worldwide. More than one million mammograms are performed each year. According to the National Breast Cancer.

There is recent evidence to suggest that salivary testing for makers of breast cancer may be used in conjunction with mammography [36-40]. Saliva-based diagnostics for the protein c-erbB-2, have great prognostic potential. Soluble fragments of the c-erbB-2 oncoprotein and the cancer antigen 15-3 were found to be significantly higher in the saliva of women who had breast cancer than in those patients with benign tumors. These initial studies indicate that the saliva test is both sensitive and reliable and can be potentially useful in initial detection and follow-up screening for breast cancer. However, to fully realize the potential of salivary biomarkers, technologies are needed that will enable facile, sensitive, specific detection of breast cancer.

http://dx.doi.org/10.5772/50351

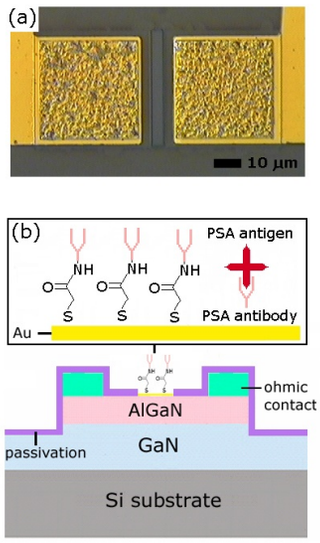

Figure 9. Schematic of HEMT sensor functionalized for PSA detection.

Antibody-functionalized Au-gated AlGaN/GaN high electron mobility transistors (HEMTs) show promise for detecting c-erbB-2 antigen [41]. The c-erbB-2 antigen was specifically recognized through c-erbB antibody, anchored to the gate area. We investigated a range of clinically relevant concentrations from 16.7 μg/ml to 0.25 μg/ml. The Au surface was functionalized with a specific bi-functional molecule, thioglycolic acid. We anchored a self-assembled monolayer of thioglycolic acid, $HSCH_2COOH$, an organic compound and containing both a thiol (mercaptan) and a carboxylic acid functional group, on the Au surface in the gate area through strong interaction between gold and the thiol-group of the thioglycolic acid. The device was incubated in a phosphate buffered saline (PBS) solution of 500 μg/ml c-erbB-2 monoclonal antibody for 18 hours before real time measurement of c-erbB-2 antigen.

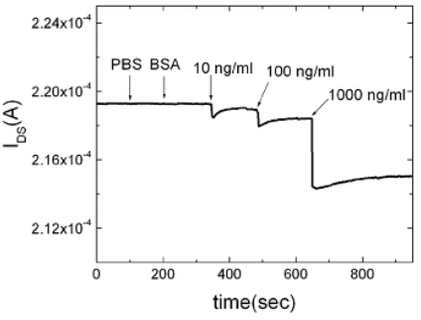

Figure 10. Drain current versus time for PSA detection when sequentially exposed to PBS, BSA, and PSA.

Figure 11 (left) shows real time c-erbB-2 antigen detection in PBS buffer solution using the source and drain current change with constant bias of 500 mV. No current change can be seen with the addition of buffer solution around 50 seconds, showing the specificity and stability of the device. The current change showed a rapid response in less than 5 seconds when tar-

get 0.25 μg/ml c-erbB-2 antigen was added to the surface. The source-drain current change was nonlinearly proportional to c-erbB-2 antigen concentration, as shown in Figure 11 (right). Between each test, the device was rinsed with a wash buffer of pH 6.0 phosphate buffer solution to strip the antibody from the antigen. Clinically relevant concentrations of the c-erbB-2 antigen in the saliva and serum of normal patients are 4-6 μg/ml and 60-90 μg/ml respectively. For breast cancer patients, the c-erbB-2 antigen concentrations in the saliva and serum are 9-13 μg/ml and 140-210 μg/ml, respectively. Our detection limit suggests that HEMTs can be easily used for detection of clinically relevant concentrations of biomarkers.

(iv) Lactic Acid

Interest in developing improved methods for detecting lactic acid has been increasing due to its importance in clinical diagnostics, sports medicine, and food analysis. An accurate measurement of the concentration of lactate acid in blood is critical to patients that are in intensive care or undergoing surgical operations as abnormal concentrations may lead to shock, metabolic disorder, respiratory insufficiency, and heart failure. The concentration of lactate in human blood is typically 1~2 mmol/L at rest, but can rise to greater than 20mmol/L during various physiological and pathophysiological states, including intense exercise, shock (e.g., hypovolemia, congestive heart failure, septic shock), infections, respiratory insufficiency, and various metabolic disorders (e.g., inborn errors of metabolism such as congenital lactic acidosis). Since elevated concentrations of lactate may not only indicate the presence but also the severity of these clinically important disorders, accurate measurements of blood lactate concentration is critical to their proper management. Lactic acid concentrations can be used to monitor the physical condition of patients with chronic diseases such as heart failure, diabetes and/or chronic renal failure.

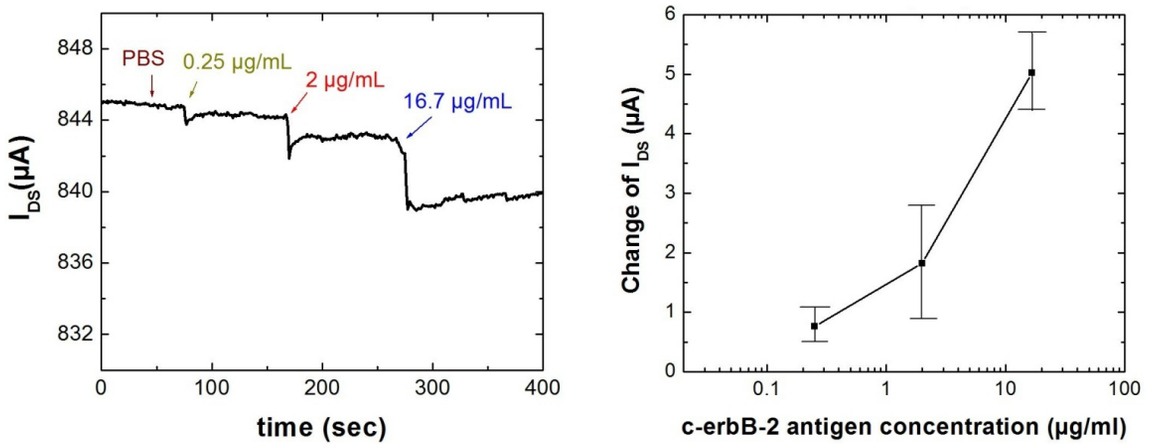

Figure 11. Drain current of an AlGaN/GaN HEMT over time for c-erbB-2 antigen from 0.25 μg/ml to 17 μg/ml (left) and change of drain current versus different concentrations from 0.25 μg/ml to 17 μg/ml of c-erbB-2 antigen.

A ZnO nanorod array, which was used to immobilize lactate oxidase oxidase (LOx), was selectively grown on the gate area using low temperature hydrothermal decomposition (Figure 12, top) [42,43]. The array of one-dimensional ZnO nanorods provided a large effective surface area with high surface-to-volume ratio and a favorable environment for the immobi-

http://dx.doi.org/10.5772/50351

lization of LOx. The AlGaN/GaN HEMT drain-source current showed a rapid response when various concentrations of lactate acid solutions were introduced to the gate area of the HEMT sensor. The HEMT could detect lactic acid concentrations from 167 nM to 139 μM. Figure 12 (bottom) shows a real time detection of lactic acid by measuring the HEMT drain current sensor to solutions with different concentrations of lactic acid. The sensor was first exposed to 20 μl of 10 mM PBS and no current change could be detected with the addition of 10 μl of PBS at approximately 40 seconds, showing the specificity and stability of the device. A rapid increase in the drain current was observed when target lactic acid was introduced to the device surface. The sensor was continuously exposed to lactic acid concentrations from 167 nM to 139 μM.

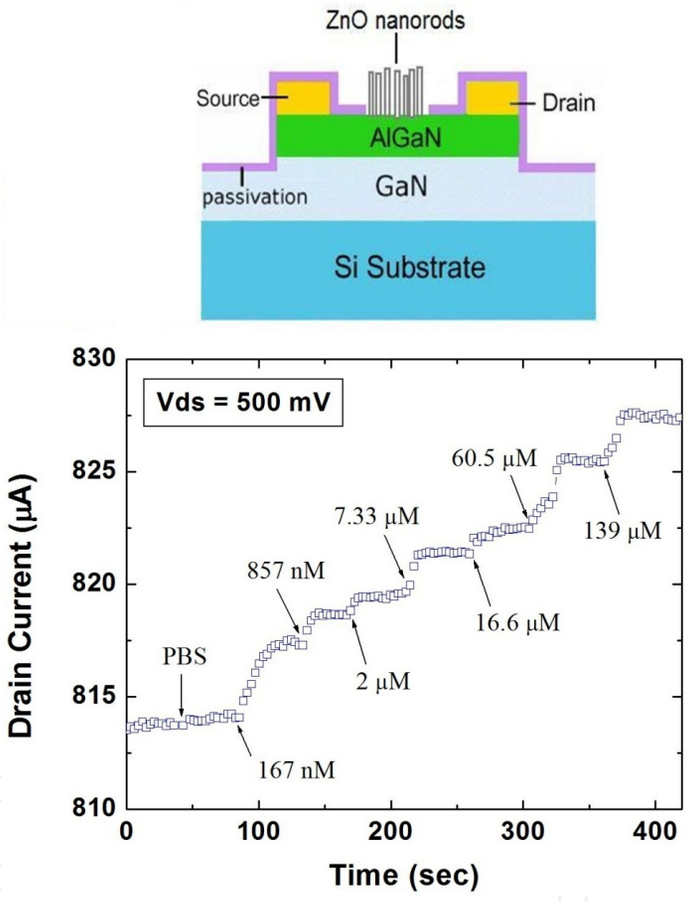

Figure 12. Schematic cross sectional view of the ZnO nanorod gated HEMT for lactic acid detection (top) and plot of drain current versus time with successive exposure to lactic acid from 167 nM to 139 μM (bottom).

(v) Chloride Ion Detection

Chloride ions are also an essential counter-ion in our bodies [44-47]. Our kidneys balance the chloride in body fluids, such as serum, blood, urine, and exhaled breath condensate (EBC). Abnormal chloride ion concentration in serum may serve as an indicator for diseases such as renal diseases, adrenalism, and pneumonia. Chloride ion concentration can be a biomarker for the level of pollen exposure in allergic asthma, chronic cough, and airway acidifi-

cation related to respiratory disease. Also, the Cl^- concentration in EBC can be used as a reference for the other biomarkers in the EBC to estimate the dilution effect from the humidity in the ambient during the EBC collection.

Current analytical methods for measuring chloride ion include colorimetry, ion-selective electrode, x-ray fluorescence spectrometry, activation analysis, and ion chromatography. However, these methods involve high expertise levels and require expensive instruments that cannot be readily transported. The narrow gap semiconductor InN has positively charged surface donor states that function as fixed surface sites for the reversible anion coordination and it has been proposed as a useful material for sensing applications. InN thin film based potentiometric ion-selective sensors have been reported to detect Cl^- ions down to 1mM. In addition, HEMTs with a Ag/AgCl gate are found to exhibit significant changes in channel conductance upon exposing the gate region to various concentrations of chorine ion solutions. The Ag/AgCl gate electrode, prepared by potentiostatic anodization, changed electrical potential when it encountered chorine ions. The HEMT shown schematically in Figure 13 (top) source-drain current showed a clear dependence on the chorine concentration.

Figure 13 (bottom) shows the time dependence of Ag/AgCl HEMT drain current at a constant drain bias voltage of 500mV during exposure to solutions with different chlorine ion concentrations. The HEMT sensor was first exposed to DI water and no change of the drain current was detected with the addition of DI water at 100 seconds. There was a rapid response of HEMT drain current observed in less than 30 seconds when target of 10^{-8} M NaCl solution was switched to the surface at 175 sec. The limit of detection of this device was 10^{-8} M chlorine in DI-water. Between each test, the device was rinsed with DI water. These results suggest that our HEMT sensors are recyclable with simple DI water rinse.

Real time detection of chloride ion detection with AlGaN/GaN high electron mobility transistors (HEMTs) with an InN thin film in the gate region has also been demonstrated [45]. The sensor, shown schematically in Figure 14, exhibited significant changes in channel conductance upon exposure to various concentrations of NaCl solutions. The InN thin film provided fixed surface sites for reversible anion coordination. The sensor was tested over the range of 100nM to 100μM NaCl solutions. Figure 14 also shows the results of real time detection of Cl^- ions by measuring the HEMT drain current at a constant drain bias voltage of 500mV during exposure to solutions of different chloride ion concentrations. No change of the drain current was detected with the addition of DI water at 100 seconds. The small spike in the current is due to mechanical disturbance of the HEMT surface when the water was added. A rapid response of drain current was observed in less than 20 seconds when target of 100 nM NaCl solution was exposed to the surface at 200 seconds. The abrupt current change stabilized after the sodium chloride solution thoroughly diffused into water and reached a steady state. When the InN gate metal encountered chloride ion, the electrical potential of the gate was changed and resulted in the increase the pizeo-induced charge density in the HEMT channel. The measured drain current of the InN gated AlGaN/GaN HEMT in NaCl solutions was linearly proportional to the logarithm of chloride concentration, satisfying the Nernst equation. The pH value of the solutions did not affect the chloride ion concentration measurements.

http://dx.doi.org/10.5772/50351

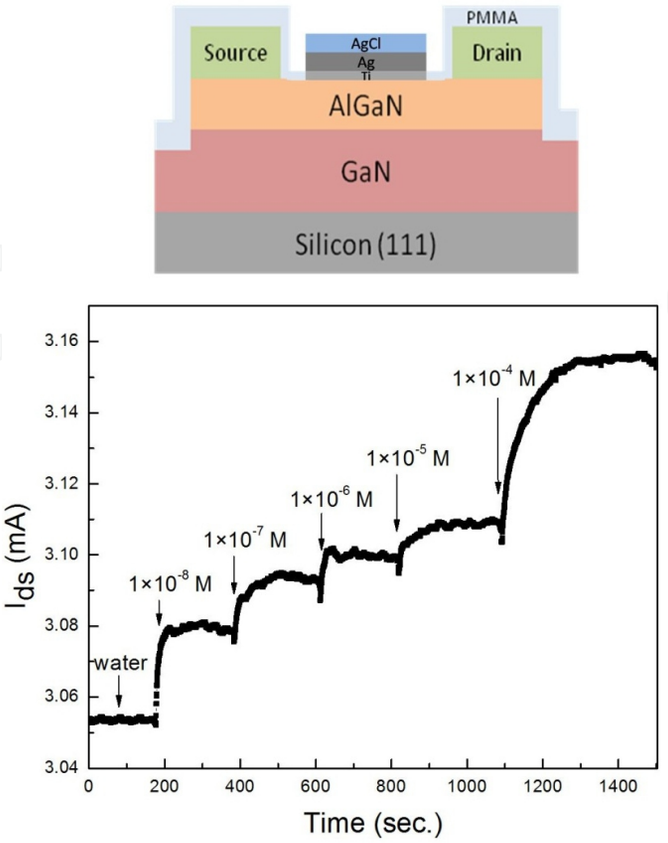

Figure 13. Schematic cross sectional view of a Ag/AgCl gated HEMT (top) and time dependent drain current of a Ag/AgCl gated AlGaN/GaN HEMT exposed to different concentrations of NaCl solutions (bottom).

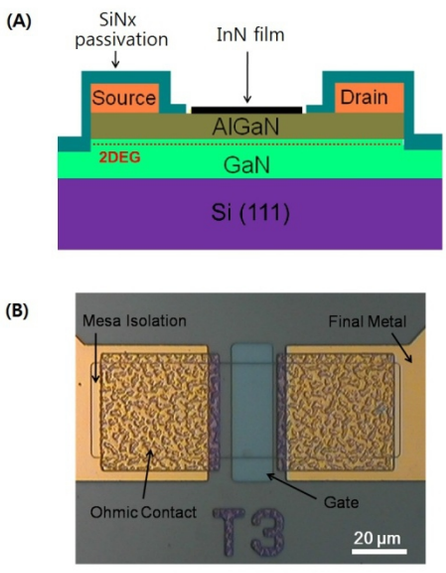

Figure 14. Schematic of an InN-gated HEMT sensor (top) and optical image of the gate region (bottom).

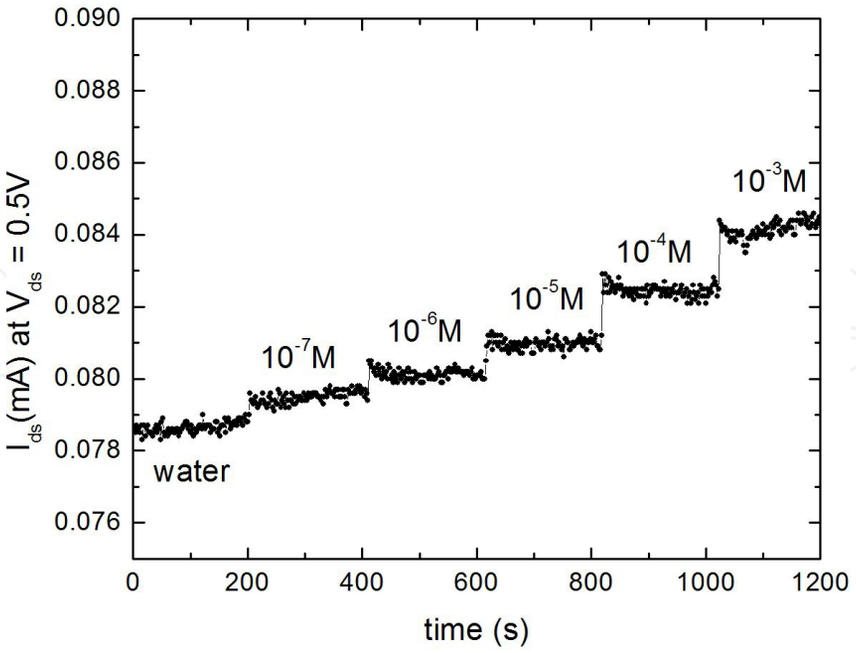

Figure 15. Source-drain current of InN-gated HEMT as different concentrations of Cl- ions were added.

(vi) Endocrine Disrupters

There have been many reports evaluating the adverse effects of endocrine disrupters (ED) on reproduction in wild animals, especially in aquatic environments [47-53]. A wide range of chemicals are considered EDs, including naturally occurring or improperly disposed estrogens and anthropogenic chemicals that were heavily used in the past. These chemicals promote feminization in wild life and also pose a threat to public health. Some reports suggest that ED can influence fetal development or act as a carcinogen. It is beneficial to develop tools that could accurately monitor the level of ED exposure.

Vitellogenin (Vtg) is a major egg yolk precursor protein used as a biomarker to indicate an organism's exposure to ED. The gene for this protein is expressed in the liver of oviparous animals under the control of estrogen. Male fish, under natural conditions, should have very low doses of Vtg since they do not produce eggs. However, if male fish are exposed to estrogen or to estrogen mimics in the environment, the Vtg gene is turned on. The dynamic range of this protein in normal male fish is 10-50 ng/ml in plasma and ~20 mg/ml in females producing eggs. There have been reports of finding as much as 100 mg/ml in some fish that were induced with estrogen. While the dynamic range is over 6 orders of magnitude, one normally finds 1~100 μg/ml in plasma in exposed males. Although Vtg from one species is limited in its application as a probe for another, some segments of Vtg are highly conserved among species, suggesting the possibility of developing antibodies with wide cross-reactivity. There have been few reports on the detection of analytes in a real solution such as serum. We have detected Vtg in both fish serum and phosphate buffer saline (PBS) using HEMT sensors with anti-vitellogenin antibodies attached to the gate region. A schematic of the sensor is shown in Figure 16.

http://dx.doi.org/10.5772/50351

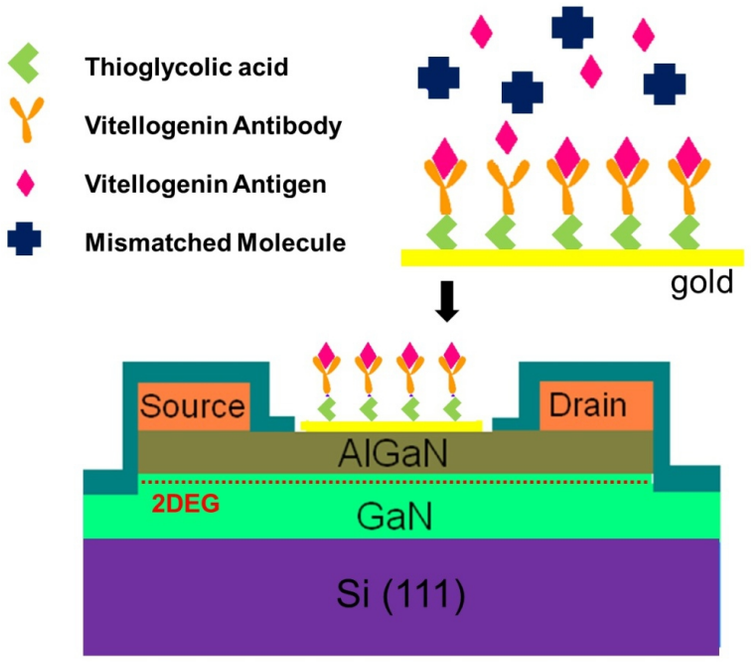

Figure 16. Cross sectional schematic of the vitellogenin-functionalized HEMT sensor.

Figure 17 shows the results of real time detection of Vtg. The drain current measurement began with 10 μL of PBS placing on the HEMT surface. Before introducing the Vtg solutions, an additional 1μL drop of PBS was added to the sensor. In comparison, a rapid response of HEMT drain current was observed in less than 10 seconds when the sensor was exposed to 5μg/mL of Vtg at 100 seconds. The abrupt current change stabilized after the VTG thoroughly diffused into the solution and reached a steady state. A larger signal change was observed when 10μg/mL of Vtg was added at 200 seconds. The sensor was exposed to higher Vtg concentrations of 50μg/mL and 100μg/mL sequentially for further real time test. The sensors were rinsed with 10mM PBS at pH=6 because antibodies have optimal reactivity at pH=7.4 and will release the antigen at a lower pH.

Perkinsus marinus (P. marinus), a protozoan pathogen of the oyster, is highly prevalent along the east coast of the United States. Perkinsus species (Perkinsozoa, Alveolata) are the causative agents of perkinsosis in a variety of mollusc species. Perkinsus species infections cause widespread mortality in both natural and farm-raised oyster populations, resulting in severe economic losses for the shellfish industry and detrimental effects on the environment. Currently, the standard diagnostic method for Perkinsus species infections has been fluid thioglycollate medium (FTM) assay detection. However, this method of detection requires several days. The polymerase chain reaction (PCR)-based technique is also used to diagnose Perkinsus, but it is quite expensive and time-consuming, and requires exquisite controls to assure specificity and accuracy. Clearly, such methods are slow and impractical in this age of global trade that requires rapid detection of such pathogens.

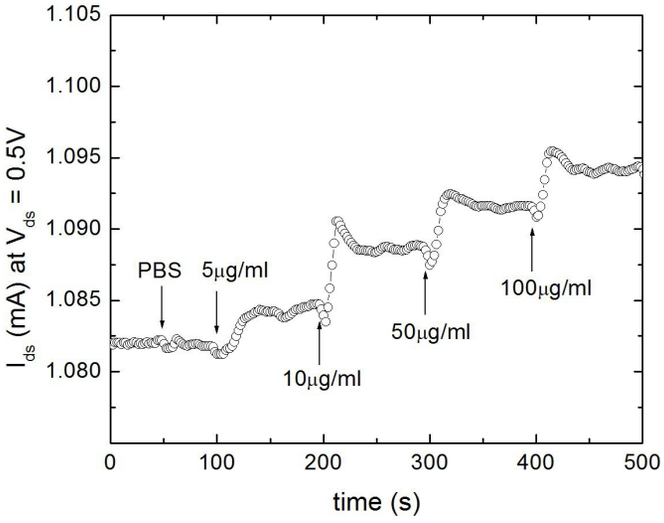

Figure 17. Real time source-drain current of sensors when introduced to 5, 10, 50, and 100 μg/mL of vitellogenin.

Figure 18 (top) shows a schematic device cross section with immobilized thioglycolic acid, and followed by anti-P. marinus antibody coating. Figure 18 (bottom) shows a picture of *Tridacna crocea*. The *Tridacna crocea* are extremely popular ornamental reef clams imported in huge numbers into the USA from the Indo-Pacific for the aquarium trade. *Tridacna crocea* are known to be vulnerable to P. marinus. This may pose a threat to domestic shellfish and negatively impact our desirability as trade partners. The infection status of the *Tridacna crocea* in this study was verified by histopathology, FTM, and polymerase chain reaction assays.

Figure 19 shows real time P. marinus detection using source and drain current change with constant drain bias of 500 mV. No current change can be seen with the addition of buffer solution mixed showing the specificity and stability of the device. The current change showed a rapid response in less than 5 seconds when 2 ul of tank 2 water was added to the surface. Continuous 2 ul of the tank 2 water added into a buffer solution resulted in further decreases of drain current. Tank 2 housed sick and dying calms releasing P. marinus organisms into the water, which subsequently shed surface antigens readily detected by the sensors. Then, the sensor was washed with PBS (pH 6.5) and used to detect the P. marinus again. The recycled sensor still showed very good sensitivity as previously. These results demonstrated real-time P. marinus detection and reusability of the sensor.

7. Summary and Conclusions

We have summarized recent progress in AlGaN/GaN HEMT sensors. These devices take advantage of microelectronics, including high sensitivity, possibility of high-density integration, and mass manufacturability. The goal is to realize real-time, portable and inexpensive chemical and biological sensors and to use these as handheld exhaled breath, saliva, urine, or blood monitors with wireless capability. Frequent screening can catch the early development of diseases, reduce the suffering of the patients due to late diagnoses, and lower the medical cost.

http://dx.doi.org/10.5772/50351

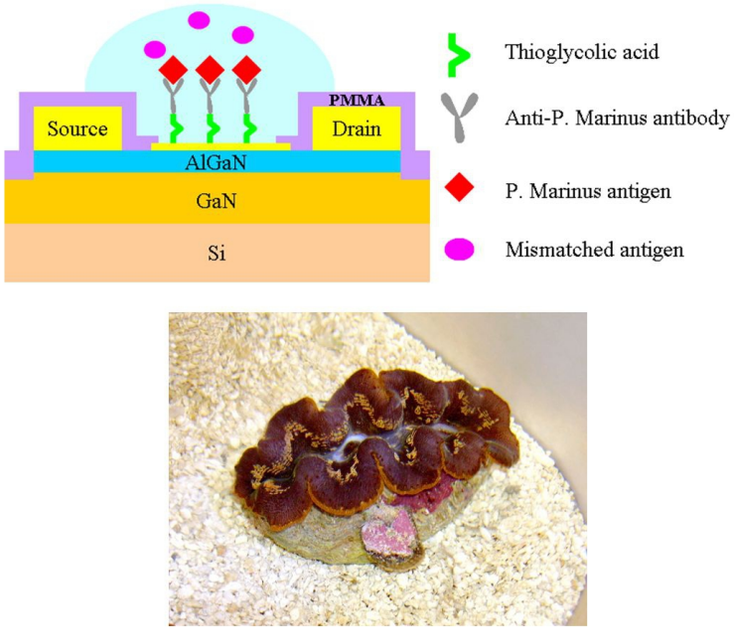

Figure 18. (top) Schematic of AlGaN/GaN HEMT sensor. The gate area was functionalized with anti-P. marinus antibody on thioglycolic acid. (bottom) A picture of the clam, which may carry the perkinsus.

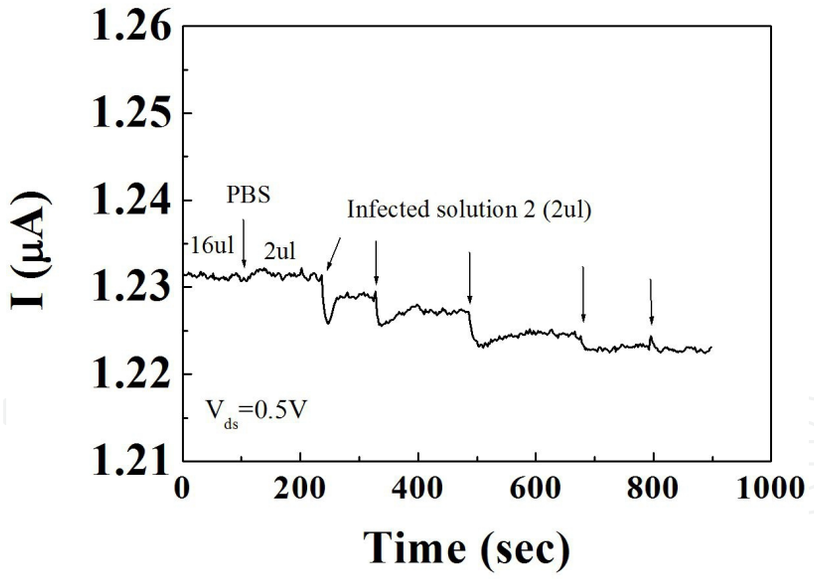

Figure 19. Real-time detection of P. marinus in an infected water from tank 2 before recycling the sensor with PBS wash (bottom).

There are many possible applications, including diabetes/glucose testing, hydrogen sensors, breast cancer testing, asthma testing, prostate testing and narcotics testing. The characteristics of these sensors include fast response (liquid phase-5 to 10 seconds and gas phase- millisecond), digital output signal, small device size (less than 100 × 100 μm^2) and chemical and thermal stability.

There are still some issues. First, the sensitivity needs to be improved to allow sensing in real body fluids, including blood and urine. Second, integrating multiple sensors on a single chip with automated fluid handling and algorithms is needed to analyze multiple detection signals. Third, a package that will result in a cheap product is needed. Fourth, the stability of surface functionalization layers in some cases is not conducive to long-term storage and this will limit the applicability of those sensors outside of clinics. There is a need for detection of multiple analytes simultaneously. However, there are many such approaches and acceptance from the clinical community is generally slow for regulatory concerns.

Acknowledgements

This work is supported by NSF. Collaborations with T. Lele, Y. Tseng, D. Dennis, W. Tan, B.P. Gila, W. Johnson and A. Dabiran are greatly appreciated.

Author details

Stephen J. Pearton[1*], Fan Ren[2] and Byung Hwan Chu[2]

*Address all correspondence to: spear@mse.ufl.edu

1 Department of Materials Science and Engineering, University of Florida, Gainesville, FL USA

2 Department of Chemical Engineering, University of Florida, Gainesville, FL USA

References

[1] Chemical Sensors (US industry forecasts for 2014 & 2019); Group, T. F., Ed.; http://www.the-infoshop.com/report/fd139268-us-chemical-sensor.html.

[2] Greenfield, R. A., Brown, B. R., Hutchins, J. B., Iandolo, J. J., Jackson, R., Slater, L., & Bronze, M. S. (2002). *The American J. Of The Medical Sciences*, 323(326), 326-332.

[3] Kang, B. S., Wang, H. T., Lele, T. P., Ren, F., Pearton, S. J., Johnson, J. W., Rajagopal, P., Roberts, J. C., Piner, E. L., & Linthicum, K. J. (2007). *Appl. Phys Lett.*, 91, 112106-112108.

[4] Wang, H. T., Kang, B. S., Chancellor, T. F., Jr., Lele, T. P., Tseng, Y., Ren, F., Pearton, S. J., Johnson, J. W., Rajagopal, P., Roberts, J. C., Piner, E. L., & Linthicum, K. J. (2007). *Appl. Phys. Lett.*, 91, 042114-042116.

[5] Kang, B. S., Wang, H. T., Ren, F., Gila, B. P., Abernathy, C. R., Pearton, S. J., Dennis, D. M., Johnson, J. W., Rajagopal, P., Roberts, J. C., Piner, E. L., & Linthicum, K. J. (2008). *Electrochem. Solid-State Lett.*, 11, J19-J21.

[6] Kang, B. S., Wang, H. T., Ren, F., Gila, B. P., Abernathy, C. R., Pearton, S. J., Johnson, J. W., Rajagopal, P., Roberts, J. C., Piner, E. L., & Linthicum, K. J. (2007). *Appl. Phys. Lett.*, 91, 012110-012112.

[7] Kang, B. S., Pearton, S. J., Chen, J. J., Ren, F., Johnson, J. W., Therrien, R. J., Rajagopal, P., Roberts, J. C., Piner, E. L., & Linthicum, K. J. (2006). *Appl. Phys. Lett.*, 89, 122102-122104.

[8] Kang, B. S., Ren, F., Wang, L., Lofton, C., Tan, W., Pearton, S. J., Dabiran, A., Osinsky, A., & Chow, P. P. (2005). *Appl. Phys. Lett.*, 87, 023508-023510.

[9] Kang, B. S., Wang, H., Ren, F., Pearton, S. J., Morey, T., Dennis, D., Johnson, J., Rajagopal, P., Roberts, J. C., Piner, E. L., & Linthicum, K. J. (2007). *Appl. Phys. Lett.*, 91, 252103-252105.

[10] Pearton, S. J., Kang, B. S., Kim, S., Ren, F., Gila, B. P., Abernathy, C. R., Lin, J., & Chu, S. N. G. (2004). *J. Phys: Condensed Matter*, 16, R961-985.

[11] Chang, J. F., Kuo, H. H., Leu, I. C., & Hon, M. H. (1994). *Sensors and Actuators*, B84, 258-261.

[12] Logothetis, E. M. (1991). Automotive oxygen sensors. *in: N. Yamazoe (Ed.), Chemical Sensor Technology*, 3, Elsevier, Amsterdam.

[13] Xu, Y., Zhou, X., & Sorensen, O. T. (2000). *Sens. Actuators*, B65, 2-9.

[14] Castañeda, L. (2007). *Materials Science and Engineering*, B 139, 149-157.

[15] Gerblinger, J., Lohwasser, W., Lampe, U., & Meixner, H. (1995). *Sens. Actuators*, B26, 93-98.

[16] Sotter, E., Vilanova, X., Llobet, E., Vasiliev, A., & Correig, X. (2007). *Sens. Actuators*, B127, 567-572.

[17] Wang, Yu-Lin., Covert, L. N., Anderson, T. J., Lim, Wantae., Lin, J., Pearton, S. J., Norton, D. P., Zavada, J. M., & Ren, F. (2007). *Electrochemical and Solid-State Letters*, 11(3), H60-H62.

[18] Wang, Y.-L., Ren, F., Lim, W., Norton, D. P., Pearton, S. J., Kravchenko, I. I., & Zavada, J. M. (2007). *Appl. Phys. Lett.*, 90, 232103-232105.

[19] Wormhoudt, J. (1985). *Infrared Methods for Gaseous Measurements*, Marcel Dekker, New York.

[20] Manuccia, T. J., & Eden, J. G. (1985). *Infrared optical measurement of blood gas concentrations and fiber optical catheter*, U.S. Patent 4,509,522.

[21] Vasiliev, A., Moritz, W., Fillipov, V., Bartholomäus, L., Terentjev, A., & Gabusjan, T. (1998). *Sens. Actuators*, B49, 133-138.

[22] Savage, S. M., Konstantinov, A., Saroukan, A. M., & Harris, C. (2000). *Proc. ICSCRM'99*, 511-515.

[23] Mitzner, K. D., Sternhagen, J., & Galipeau, D. W. (2003). *Sensors and Actuators*, B9, 92-97.

[24] Wollenstein, J., Plaza, J. A., Cane, C., Min, Y., Botttner, H., & Tuller, H. L. (2003). *Sensors and Actuators*, B93, 350-356.

[25] Hu, Y., Zhou, X., Han, Q., Cao, Q., & Huang, Y. (2003). *Mat.Sci.Eng.*, B99, 41-46.

[26] Ling, Z., Leach, C., & Freer, R. (2001). *J.European Ceramic Society*, 21, 1977-1981.

[27] Rao, B. B. (2000). *Materials Chem.Phys.*, 64, 62-67.

[28] Mitra, P., Chatterjee, A. P., & Maiti, H. S. (1998). *Mater. Lett.*, 35, 33-38.

[29] Chang, C. Y., Kang, B. S., Wang, H. T., Ren, F., Wang, Y. L., Pearton, S. J., Dennis, D. M., Johnson, W., Rajagopal, P., Roberts, J. C., Piner, E. L., & Linthicum, K. J. (2008). *Appl.Phys. Lett.*, 92, 232102.

[30] Thomson, I. M., & Ankerst, D. P. (2007). *CMAJ*, 176, 1853-1857.

[31] Wang, Y. L., Chu, B. H., Chen, K. H., Chang, C. Y., Lele, T. P., Tseng, Y., Pearton, S. J., Ramage, J., Hooten, D., Dabiran, A., Chow, P. P., & Ren, F. (2008). *Appl. Phys. Lett.*, 93, 262101-262103.

[32] Kang, B. S., Wang, H. T., Ren, F., & Pearton, S. J. (2008). *J. Appl. Phys.*, 104, 031101-031103.

[33] American Cancer Society. (2007, 08 Nov.) *Detailed Guide: Prostate Cancer. What Are the Key Statistics About Prostate Cancer*, http://www.cancer.org/docroot/CRI/content/CRI_2_4_1X_What_are_the_key_-statistics_for_prostate_cancer_36.asp?rnav=cri.

[34] Wang, J. (2006). *Biosens. Bioelectron.*, 21, 1887-1994.

[35] United States Department of Health and Human Services. (2007, 3 Nov.) *What is Breast Cancer?*, http://www.hhs.gov/breastcancer/whatis.html.

[36] Michaelson, J. S., Halpern, E., & Kopans, D. B. (1999). *Radiology*, 212(2), 551-558.

[37] Harrison, T., Bigler, L., Tucci, M., Pratt, L., Malamud, F., Thigpen, J. T., Streckfus, C., & Younger, H. (1998). *Spec. Care Dentist*, 18(3), 109-115.

[38] Mclntyre, R., Bigler, L., Dellinger, T., Pfeifer, M., Mannery, T., & Streckfus, C. (1999). *Oral Surg. Oral Med. Oral Pathol. Oral Radiol. Endod.*, 88(6), 687-695.

[39] Streckfus, C., Bigelr, L., Dellinger, T., Pfeifer, M., Rose, A., & Thigpen, J. T. (1999). *Clin. Oral Investig.*, 3(3), 138-144.

[40] Streckfus, C., Bigler, L., Dellinger, T., Dai, X., Kingman, A., & Thigpen, J. T. (2000). *Clin Cancer Res.*, 6(6), 2363-2368.

[41] Chen, K. H., Kang, B. S., Wang, H. T., Lele, T. P., Ren, F., Wang, Y. L., Chang, C. Y., Pearton, S. J., Dennis, D. M., Johnson, J. W., Rajagopal, P., Roberts, C., Piner, E. L., & Linthicum, K. J. (2008). *Appl. Phys. Lett.*, 92, 192103.

[42] Chu, B. H., Kang, B. S., Ren, F., Chang, C. Y., Wang, Y. L., Pearton, S. J., Glushakov, A. V., Dennis, D. M., Johnson, J. W., Rajagopal, P., Roberts, J. C., Piner, E. L., & Linthicum, K. J. (2008). *Appl. Phys. Lett.*, 93, 042114-042116.

[43] Heo, Y. W., Norton, D. P., Tien, L. C., Kwon, Y., Kang, B. S., Ren, F., Pearton, S. J., & La Roche, J. R. (2004). *Mat. Sci. Eng.*, R47, 1-51.

[44] Hung, S. C., Hicks, B., Wang, Y. L., Pearton, S. J., Dennis, D. M., Ren, F., Johnson, J. W., Rajagopal, P., Roberts, J. C., Piner, E. L., Linthicum, K. J., & Chi, G. C. (2008). *Appl. Phys. Lett.*, 92, 193903-193905.

[45] Chu, Byung-Hwan, Lin, Hon-Way, Gwo, Shangjr, Wang, Yu-Lin, Pearton, S. J., Johnson, J. W., Rajagopal, P., Roberts, J. C., Piner, E. L., Linthicuni, K. J., & Ren, Fan. (2010). *Vac. Sci. Technol.*, B28, L5-7.

[46] Shekhar, H., Chathapuram, V., Hyun, S. H., Hong, S., & Cho, H. J. (2003). *IEEE Sensors*, 1, 67-71.

[47] Taylor, J., & Hong, S. (2000). *J. Lab. Clin. Med.*, 31, 563-570.

[48] Porte, C., Janer, G., Lorusso, L. C., Ortiz-Zarragoitia, M., Cajaraville, M. P., Fossi, M. C., & Canesi, L. (2006). *Comparative Biochemistry and Physiology, Part C*, 143, 303-309.

[49] Mosconi, G., Carnevali, O., Franzoni, M. F., Cottone, E., Lutz, I., Kloas, W., Yamamoto, K., Kikuyama, S., & Polzonetti-Magni, A. M. (2002). *Gen. Comparative Endocrinology*, 126, 125-130.

[50] Sumpter, J. P., & Jobling, S. (1995, Oct.) Environmental Health Perspectives. 103(7), *Estrogens in the Environment*, 173-178.

[51] Matozzo, V., Gagné, F., Marin, M. Gabriella., Ricciardi, F., & Blaise, C. (2008). *Environment International*, 34, 531-534.

[52] Watson, C. S., Bulayeva, N. N., Wozniak, A. L., & Alyea, R. A. (2007). *Steroids*, 72, 124-128.

[53] Garcia-Reyero, N., Barber, D. S., Gross, T. S., Johnson, K. G., Sep´ulveda, M. S., Szabo, N. J., & Denslow, N. D. (2006). *Aquatic Toxicology*, 78(358), 358-362.

[54] Wang, Y.-L., Chu, B. H., Chen, K. H., Chang, C. Y., Lele, T. P., Papadi, G., Coleman, J. K., Sheppard, B. J., Dungen, C. F., Pearton, S. J., Johnson, J. W., Rajagopal, P., Roberts, J. C., Piner, E. L., & Linthicum, K. J. (2009). *Appl. Phys. Lett.*, 94, 243901-243903.

IntechOpen